Available online at www.sciencedirect.com

jmr&t
Journal of Materials Research and Technology

journal homepage: www.elsevier.com/locate/jmrt

Original Article

Value-added utilization of coal fly ash in polymeric composite decking boards

Guxia Wang [a,b], *Zhaoshuai Li* [a,b], *Jun Yan* [c], *Yongqiang Qian* [c], *Yen Wei* [c,d], *Dan Li* [c,e,**], *Shengwei Guo* [c,e,*]

[a] *Ningxia Key Laboratory of Solar Chemical Conversion Technology, School of Chemistry & Chemical Engineering, North Minzu University, Yinchuan 750021, PR China*
[b] *Key Laboratory for Chemical Engineering and Technology, State Ethnic Affairs Commission, School of Chemistry & Chemical Engineering, North Minzu University, Yinchuan 750021, PR China*
[c] *School of Materials Science & Engineering, North Minzu University, Yinchuan 750021, PR China*
[d] *Key Laboratory of Organic Optoelectronics and Molecular Engineering, Department of Chemistry, Tsinghua University, Beijing 100084, PR China*
[e] *International Scientific and Technological Cooperation Base of Industrial Solid Waste Cyclic Utilization and Advanced Materials; Key Laboratory of Polymer Materials and Manufacturing Technology, Yinchuan 750021, PR China*

ARTICLE INFO

Article history:
Received 16 November 2022
Accepted 5 February 2023
Available online 10 February 2023

Keywords:
Coal fly ash
Value-added utilization
Polyvinyl chloride
Composite materials

ABSTRACT

The value-added utilization of coal fly ash (CFA) remains a major challenge worldwide, as tens of millions of tons CFA are stockpiled or landfilled per year in China along, leading to a waste of resources and environmental pollution. Herein, a facile, environmentally friendly, and value-added strategy of combining modified CFA with polyvinyl chloride (PVC) to form CFA/PVC composites, was adopted to effectively solve the problems caused by the utilization of coal resources. In this process, the composites were prepared by hot-mixing CFA with aluminate coupling agent, PVC and additives, followed by extrusion, cooling, shaping, traction, and cutting. The resulting material with excellent mechanical properties (static bending strength, tensile strength, and hardness are 34.9 MPa, 17.1 MPa, and HRR 103, respectively) was successfully utilized as the CFA-plastic composites decking boards (CFA/PVC composites). Compared with the conventional materials for this use, our material exhibited comparable performance but is more attractive from both environmental and economical point of view. More importantly, this strategy reduces the cost for production of decking boards by 10–20%, as the process is rather simple and robust, it was industrialized.

* Corresponding author.
** Corresponding author.
E-mail addresses: lidan@nun.edu.cn (D. Li), shengwei@nun.edu.cn (S. Guo).
https://doi.org/10.1016/j.jmrt.2023.02.026

1. Introduction

Coal fly ash (CFA), a powder-like solid waste captured from effluent gas of coal-fired thermal power plants during coal combustion [1–3]. The chemical composition of CFA is very complex, essentially contains SiO_2, Al_2O_3, Fe_2O_3, CaO, MgO and Na_2O [4,5]. China is the largest coal consumer around the world, and coal accounts for more than 60% of its energy consumption structure [6,7]. Four tons of coal burning produces one tons of CFA. Consequently, CFA currently remains one of the largest solid wastes in China [2]. Owing to its insufficient utilization rate, only about 70%, the total accumulated CFA has exceeded 3 billion tons [8]. If not properly disposed off, it can cause serious waste of land resources and environmental pollution [9], because of CFA contains a variety of heavy metal admixtures [4,10]. And one of the main factors hindering the use of CFA is the regional imbalance in supply and demand [8]. Continue to improve the utilization of CFA, and transform trash to treasure, is one of the urgent scientific issues in China.

Chinese government have been vigorously promoting resource utilization of CFA in various fields. Currently, CFA in China mainly serves as paving, mine backfilling, cement raw materials, concrete, and low-end building materials. When mechanically activated CFA is introduced to cement or concrete, the mechanical strength and durability are improved significantly [11,12]. In fact, CFA-based hollow block [13,14], CFA-based permeable brick [15] and CFA-based insulation board [16] are quite popular in China due to simple process and low cost. Over the past few years, new directions in CFA utilization including catalyst carrier [17], CFA/polymer composites electrolyte of all-solid-state lithium batteries [18], CFA-based agricultural melioration, solid sorbents for hydrogen storage [19] enhancers for polyvinyl chloride dichlorination [20] broad band microwave absorber [21] treatment of wastewater [22–24] and high-volume CFA concrete production are attracting attention from academic and industrial circles.

Polyvinyl chloride (PVC) is a common plastic, and widely used in all aspects of production and daily life due to its good quality [25]. The biggest markets are pipes and window profiles, followed by rigid films and cables. Wood powder [26,27] and $CaCO_3$ [28] often used as additives are incorporated during PVC production to improve of PVC products' mechanical properties and extensive its applications. However, using large amounts of $CaCO_3$ and wood powder produce large amounts of carbon emissions. CFA cenosphere has low specific gravity and high mechanical strength, which is a very good filler. It could replace much more expensive $CaCO_3$ and wood powder as an additive to improve the mechanical properties of the PVC plastic.

Herein, we report the production of CFA/PVC composites for CFA-plastic composite decking boards. Conventionally, the decking boards were made of composites of $CaCO_3$ and PVC where the addition of $CaCO_3$ can improve the mechanical performance [25]. Considering the low specific gravity and high mechanical strength of CFA, we expected that, it can be used as alternative for $CaCO_3$ as the filler. Considering the large market of decking boards in China, this could be a promising way to utilize the CFA. For this purpose, CFA particles were modified in-situ during mixing with the PVC by aluminate coupling agent. Then the modified CFA exhibited improved compatibility with PVC resin, compared with the pristine CFA. The composites for decking were readily obtained by extrusion and exhibited high thermal stability as well as excellent mechanical and waterproof performance. In addition to the environmental benefits, the use of CFA instead of $CaCO_3$ also reduce the cost of decking by 10–20%. Our research provides an efficient pathway for the high-value utilization of CFA.

2. Experimental section

2.1. Materials

CFA was purchased from a local coal-combustion power plant in Ningxia, China. The results of analysis of chemical composition of fly ash are summarized in Table 1. It shows that the basic components of CFA are Al determined as Al_2O_3 and Si as SiO_2. The sum of them is 67.94% of dry weight of waste. CFA contains quite large amounts of Fe determined as Fe_2O_3, Ca as CaO, Mg as MgO, K as K_2O, Na as Na_2O, Ti and P, and the CFA's loss on ignition is 5.52%. As Fig. S1 shows the main crystalline phases of CFA powder are mullite [29], quartz and a small amount of hematite crystalline phase. CFA was used as received without any additional treatment. The PVC was purchased from Yinchuan Building Materials Co., Ltd., Ningxia Shide Group. Calcium–Zinc stabilizer (Ca–Zn stabilizer, WS208–C10) used as heat stabilizer for PVC was purchased from Guangzhou Wensu additives Co., Ltd. Chlorinated polyethylene (CPE135) flexibilizer was purchased from Weihai Haida Plastic Co., Ltd. Impact modifier of acrylates copolymer (ACR, LP-812) was purchased from Shandong Ruifeng polymer material Co., Ltd. Aluminate coupling agent ($C_{39}H_{77}AlO_5$) was purchased from Nanjing Jingtianwei Chemical Co., Ltd. All materials and chemicals were used as received.

2.2. Instrumentation and characterization

The morphology of CFA particles was analyzed in the dry state by a field emission scanning electron microscopy (FE-SEM, SIGMA 500, Zeiss) and the particle size was analyzed in water by a laser particle size distribution analyzer (X100, Beijing Hanmiwanger Co., Ltd.). The aqueous solution was subjected

Table 1 – The element analysis of CFA[a].

Elements	SiO_2	Al_2O_3	Fe_2O_3	CaO	K_2O	MgO	Na_2O	TiO_2	P_2O_5	Others	LOI
Content (%)	44.28	23.66	4.3	2.61	1.1	0.78	0.5	0.691	0.102	16.46	5.52

[a] The element analysis is determined using X-ray fluorescence spectroscopy.

Fig. 1 – The preparation of CFA-based composite decking materials.

to ultrasonic for 10 min before the measurement. According to the standards DZ/T 0279.1–2016 and DZ/T 0279.10–2016, X-ray fluorescence spectrometer (DDYS-199, Mineral Resources Supervision and Testing Centre, Yinchuan, Ministry of Land and Resources) was used to analyse the CFA composition at room temperature and humidity of 17%. X-ray diffraction analysis were carried out to identify the crystalline phases of CFA by using an X-ray diffractometer (DX-2700, Dandong Haoyuan Instruments Co., Ltd.) operating at 40 kV/30 mA (Cu target; Scan range 2θ is 10–80°; Test rate is 2°/min). The infrared spectra were recorded on a Fourier transform infrared spectrometer (FTIR, WQF-520 A, Beijing Beifen Rayleigh Analytical Instrument Co., Ltd.). The materials were compressed with KBr to form tablets for the measurement. The static contact angles were measured on a dynamic contact angle measuring instruments (Shanghai Zhongchen Co., Ltd.). The thermogravimetric analysis (TGA) was performed on a comprehensive thermal analyser (NETZSCH STA 449 F3, NETZSCH-Gerätebau GmbH) at temperature ranging from 30 to 1000 °C. The differential scanning calorimetry (DSC) curves were recorded on a differential scanning calorimeter (Q20, TA) at temperature ranging from 30 to 180 °C. Both TGA and DSC were performed at a heating rate of 10 °C/min under the N_2 atmosphere.

Table 2 – Recipes of CFA-based composite decking materials with various amounts CFA.

CFA	PVC	CPE	ACR	Ca–Zn Stabilizer	Aluminate coupling agent
120	100	11	1.2	4.6	1.8
160	100	11	1.2	4.6	2.4
200	100	11	6	4.6	3.0
230	100	11	7	4.6	3.5
300	100	11	8	4.8	4.5

*Units: parts per hundred parts of resin, abbreviated as phr.

An electronic universal testing machine (UTM4304, Shenzhen Sansizhongheng Co., Ltd.) was used to measure the tension strength and the bending strength, which were measured according to GB1040.2–2006 [30–32] and GB/T9341-2000 [33], respectively. For the measurement of tension strength, samples were shaped into type I splines, and the stretching speed was 2 mm/min. In the measurement of bending strength, the size of samples, span and speed of bending were 80 × 10 × 4 mm, 64 mm, and 2 mm/min, respectively. The impact strength was measured according to GB/T1843-2008 [34,35] on an Izod impact testing machine (MZ-

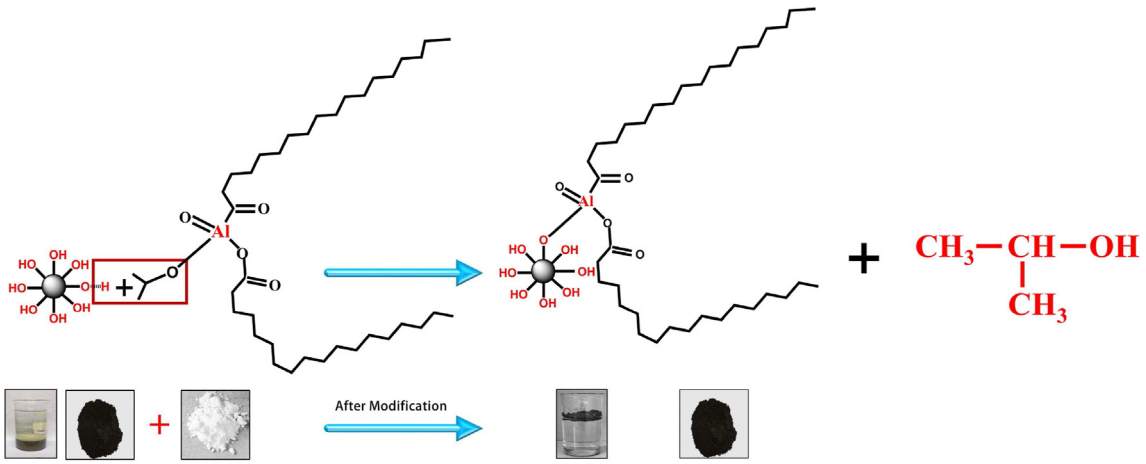

Fig. 2 – Modification of CFA by aluminate coupling agent.

2056, Jiangsu Mingzhu Co., Ltd.), where the size of samples was 80 × 10 × 4 mm. The Rockwell hardness were measured on a digital Rockwell hardness tester (HRS-150, Shanghai Lianer).

2.3. *Processing of materials*

The procedure for production of the composite is schematically shown in Fig. 1. As Table 2 shows, The PVC, CFA, Ca–Zn stabilizer, CPE, and ACR was added to the high-speed mixer (FM1000, Henschel Industrietechnik GmbH)) through the connecting pipe. The mixture was subjected to hot mixing at a temperature of 118 °C and a speed of 600–800 r/min for 5–10 min to remove most of the residual water. The aluminate coupling agent was then added to the mixture and stirring was continue for additional 10 min to yield the modified CFA, which was transferred to the cold mix pot (HM3500, Henschel Industrietechnik GmbH). The dry blend was obtained after cold mixing at 46 °C for 10–15 min.

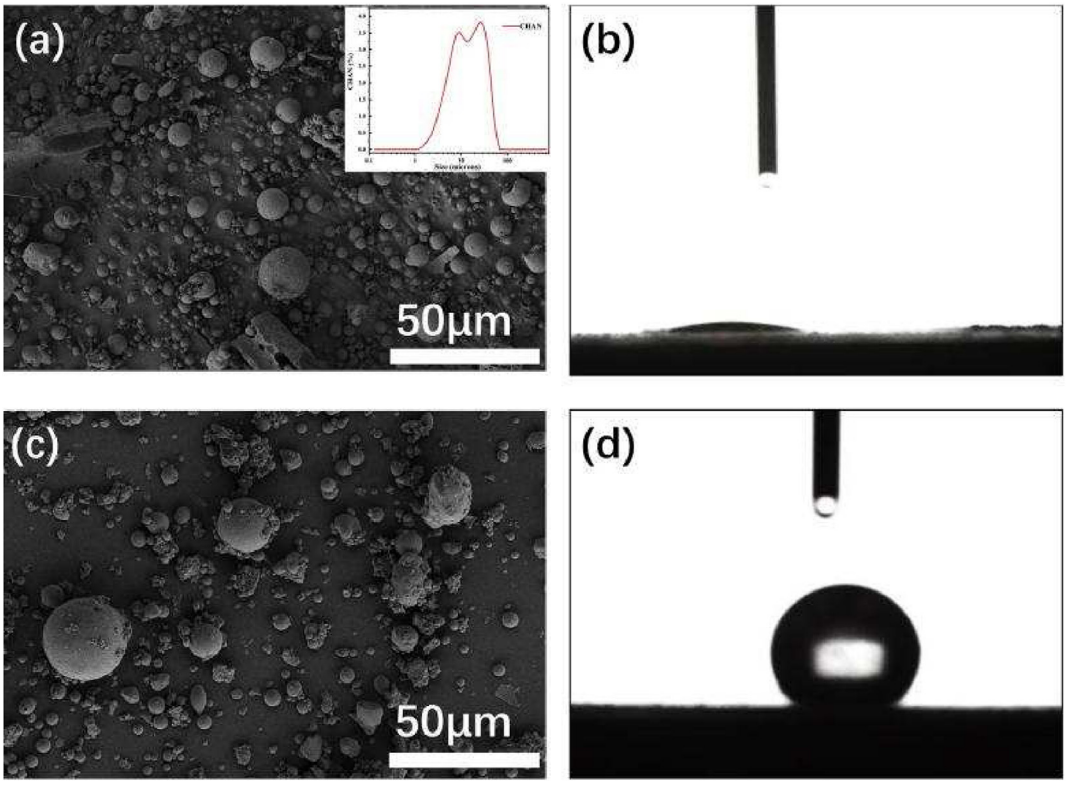

Fig. 3 – Characterization of pristine CFA by SEM (a) and contact angle (b), and characterization of modified CFA by SEM (c) and contact angle (d).

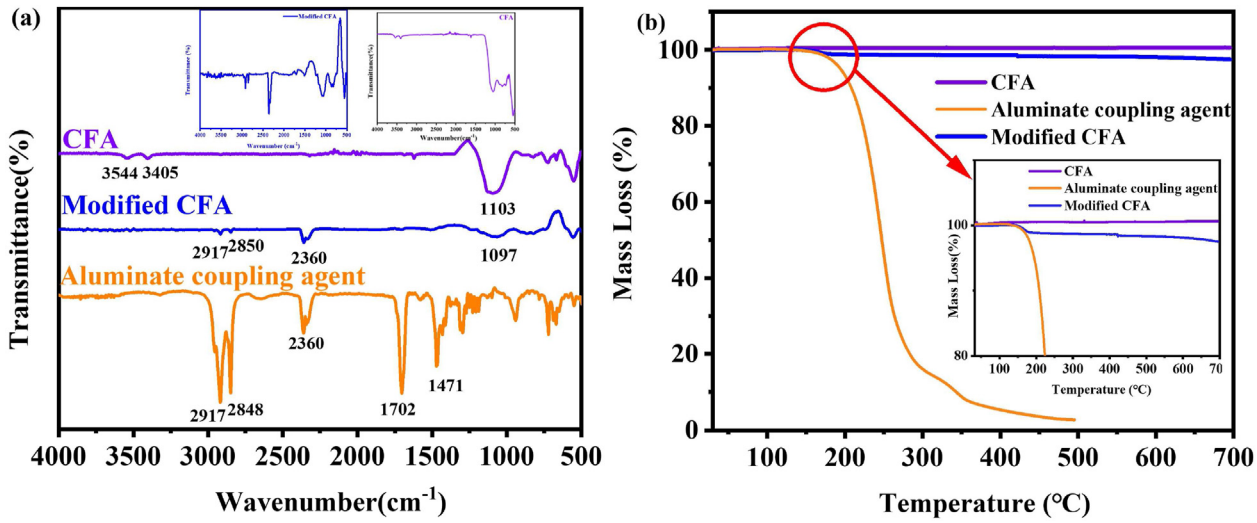

Fig. 4 – FTIR (a) and TGA (b) of unmodified CFA, aluminate coupling agent and modified CFA.

CFA/PVC composite decking extrusion moulding: The dry blend was added to the hopper of the extruder, and the parallel twin-screw extruder (KMD114-32, KRAUSS MAFFEI)) was used for extrusion, cool and shape, pull, and cut, and finally form the standard decking material. The screw speed of the extruder and feeding unit were 6.8 r/min and 30 r/min, respectively. The pulling speed of the pulling machine was 1.2 m/min. The pressure and temperature of the melted were 13 MPa and 180 °C, respectively. The execution temperature of each section of the barrel area were 175, 175, 175 and 173 °C, respectively. The execution temperature of the connection area was 160 °C. The execution temperature of each section of the die head were 195, 195, 195 and 195 °C, respectively.

3. Results and discussion

3.1. *CFA-plastic composites decking boards synthesis and characterization*

The hydroxyl group on the surface of CFA makes it hydrophilic and reduce the compatibility between CFA and the hydrophobic organic resin. Therefore, surface modification of CFA is required before it is used as filler [36–38]. Herein, we adopted the in-situ modification approach that convert the dry blend to products in one step (Fig. 2). This is superior over previous methods that require multi-step processing and handling, which lead to dust pollution in the workshop in practical application.

First, we characterized the size and geometry of CFA particles. As shown in Fig. 3a, the pristine CFA dispersed in water has a broad size distribution ranging from 4.23 to 40.8 μm, and the average size (D_{50}) is 13.17 μm. This was confirmed by subsequent SEM images of pristine and modified CFA, suggesting that modification did not alter the geometry and size of the CFA particles.

Next, we characterized the wettability of pristine and modified CFA by measurement of contact angle. The pristine CFA is highly hydrophilic, as the water drops spread on the surface rapidly. In contrast, on modification, the particles became rather hydrophobic [39], as characterized by a contact angle of (134 ± 2) ° (the static result of five measurement), confirming the successful of our modification strategy [36,37].

The introduction of organic thin layer onto the surface of CFA particles was further confirmed by the changes in the infrared spectra (Fig. 4a). Pristine CFA displayed characteristic band at 1103 cm^{-1}, which was assigned to the stretching vibration of -Si-O-Si- [36,40,41]. In addition to this, several bands were emerged on the modified CFA that were attribute to the introduction of organic layer. For example, the bands at 2917 and 2850 cm^{-1} were contributed by the $-CH_2-$ group [42,43], as they can also be found in the spectra of pure aluminate coupling agent. Note that, the strong band at 2360 cm^{-1} was due to the CO_2.

In addition to the introduction of organic groups, the modification by aluminate coupling agent might also cause an increase in the content of aluminum [44]. This hypothesis was

Table 3 – Elemental content before and after modification.

Comparison of elements before and after modification	Unmodified CFA (wt%)	Modified CFA (wt%)
O	54.79	54.44
Na	0.32	0.31
Mg	0.42	0
Al	17.84	18.53
Si	20.34	20.74
S	0.47	0
K	1.20	1.28
Ca	1.31	1.12
Ti	0.83	0.97
Fe	2.49	2.61
Total volume	100	100

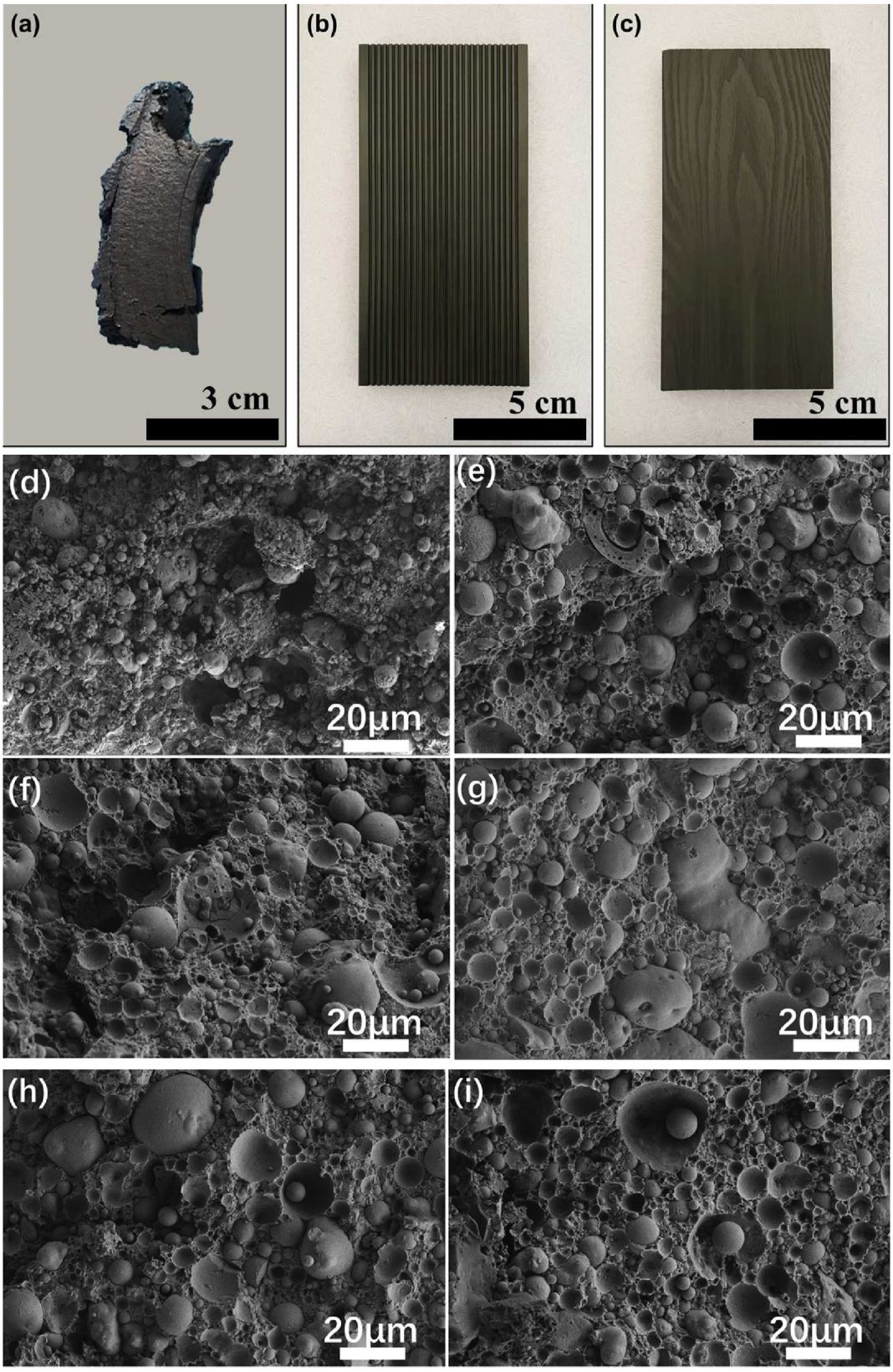

Fig. 5 – Optical images of unmodified 80 Phr CFA/PVC (a); modified CFA/PVC (b) and (c); (d) SEM images of CFA/PVC with unmodified CFA; (e)–(i) SEM images of CFA/PVC with 120, 160, 200, 230 and 300Phr CFA.

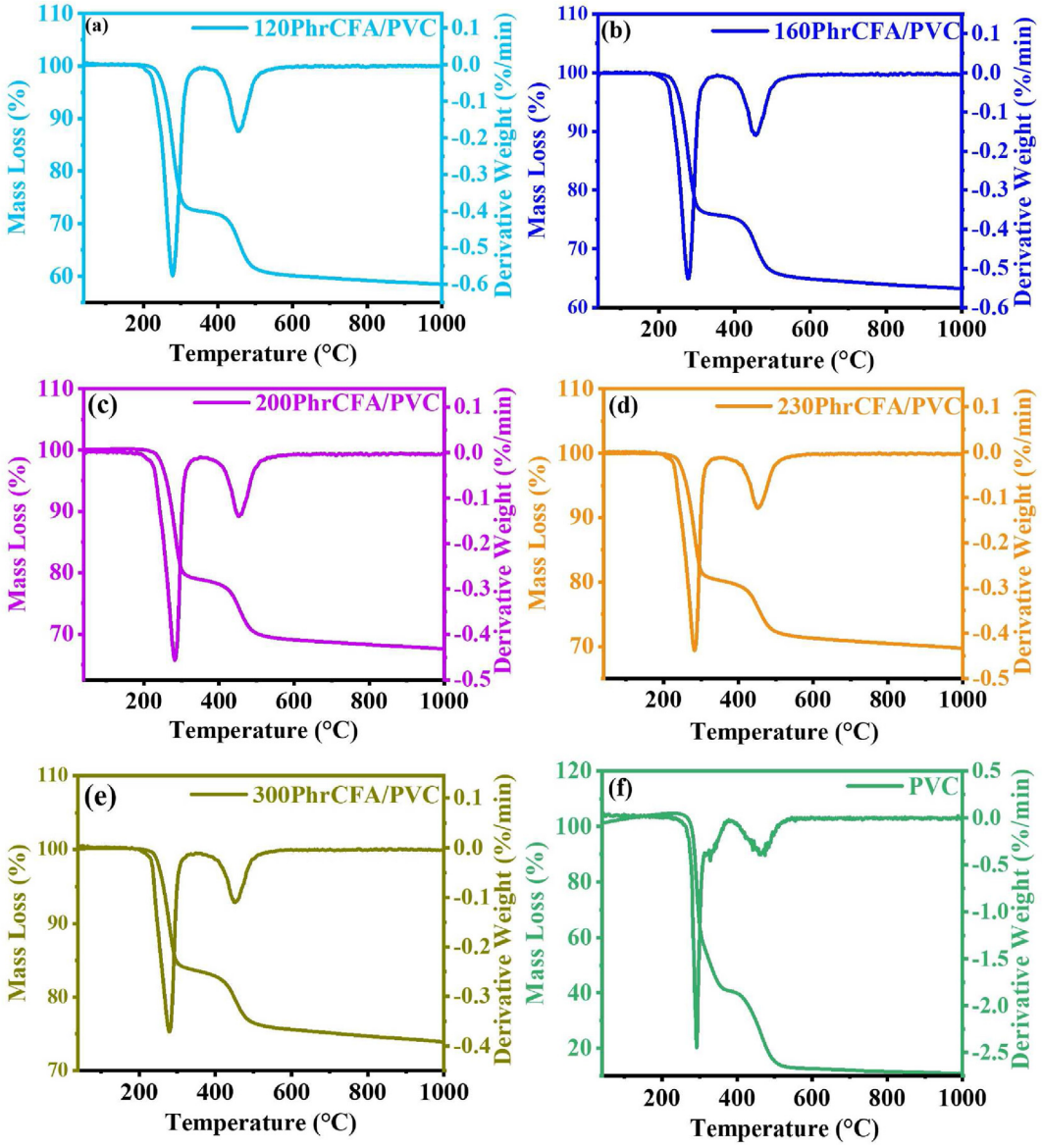

Fig. 6 – TG-DTG curves of the 120 (a), 160 (b), 200 (c), 230 (d), 300 Phr (e) CFA/PVC and PVC (f).

verified by the elemental analyses on pristine and modified CFA (Fig. S2 and Table 3). The content of Al element increases from 17.84% for pristine CFA to 18.53% for modified CFA.

Finally, we use thermal analysis to provide a semi-quantitative understanding about the quantity of organic layer on the CFA (Fig. 4b). For pristine CFA, no loss of mass can be observed at temperature below 700 °C [40,45,46]. In contrast, the pure aluminate coupling agent decomposed completely at 500 °C. Thus, the 1.4% weight loss for modified CFA at 700 °C was attributed to the organic layer [38], confirming that the aluminate coupling agent cover on the surface of CFA.

3.2. *CFA/PVC composites*

The protocol of preparing composites from CFA and PVC was described in the experimental section. Before systematically characterized the mechanical properties of the composites, we illustrated the necessity of surface modification. The decking made of PVC and pristine CFA composites has a low quality, as the surface is rough along with clearly visible cracks (Fig. 5a). At the microscopic scale, this is reflected by the phase separation between CFA and PVC (Fig. 5d). Because CFA is an inorganic substance, and PVC is organic resin. During the processing, the interface interaction between CFA and PVC resin is weakly, while CFA cannot be uniformly dispersed in PVC resin, resulting in obvious phase separation phenomenon. Although the compatibility between CFA and PVC has been improved by modification, aggregation of CFA was observed at high CFA content (Fig. 5i).

The resulting decking has a smooth surface, and neither dents nor decomposition discoloration lines can be observed (Fig. 5b and c), suggesting CFA/PVC composites as a promising material for decking boards.

Table 4 – Summary of the thermal properties of CFA/PVC composites.

Sample	First step		Second step		W (%)	T_g (°C)
	T_1 (°C)	W_1 (%)	T_2 (°C)	W_2 (%)		
120PhrCFA/PVC	280	27.8	457	13.7	41.5	83.9
160PhrCFA/PVC	277	24.0	456	12.6	36.8	82.8
200PhrCFA/PVC	284	21.0	453	11.3	32.4	82.7
230PhrCFA/PVC	282	20.0	452	10.2	30.3	83.2
300PhrCFA/PVC	279	16.5	451	9.6	26.1	83.2
PVC	293	64.0	469	30.0	94.0	86.7

T_1: The temperature corresponding to the first stage of the composites reaching the maximum mass loss; W_1: Mass loss during the first stage of decomposition of the composites; T_2: The temperature corresponding to the second stage of the composites reaching the maximum mass loss; W_2: Mass loss during the second stage of decomposition of the composites; W: Total mass loss of the composites.

To understand the composition of the CFA/PVC composite, we performed the TGA on CFA/PVC, CFA/PVC, and the PVC (Fig. 6). All samples displayed qualitatively similar TGA curves. The two characteristic stages of thermal degradation were attributed to the decomposition of PVC as reported previously [20,25,47,48]. The weight loss at first stage (W_1, 240–382 °C) and second stage (W_2, 396–516 °C) was 64% and 30%, respectively. Total weight loss (W) was 94% (Fig. 6f) [49].

We also studied the thermal degradation of composites with different CFA content (Fig. 6 and Table 3). At 120 parts of CFA (120PhrCFA/PVC), the W, W_1, and W_2 were 41.5%, 27.8% and 13.7%, respectively. The weight loss decreases as the CFA contents increase. At 300 parts of CFA (300PhrCFA/PVC), the W, W_1, and W_2 reduced to 26.1%, 16.5% and 9.6%, respectively.

The TGA curves were transformed to DTG plots to analyse the temperature with maximum thermal degradation rate at the first stage (T_1) and second stage (T_2). For PVC without addition of CFA, the T_1 and T_2 were 293 and 469 °C, respectively. The T_1 decreased by 16, 9 and 14 °C, for composites with CFA content of 160, 200 and 300 parts of CFA, respectively (Table 4). T_2 also decreased as the CFA content increased (Table 4). Therefore, addition of CFA likely accelerates the thermal degradation of PVC [48]. Therefore, the maximum CFA content for making composites was 200 parts. The reason for the decrease in thermal stability of the composites is that SiO_2 and Al_2O_3 (main chemical components in CFA) are solid acids, which are found to have catalytic ability to dichlorination of PVC [20,48,50–53]. Furthermore, CFA contains a certain amount of basic metal oxides such as CaO, K_2O, Na_2O, which has a significant adsorption effect on HCl [20]. Therefore, CFA can promote the removal of HCl in PVC matrix [20,25].

We further measured the glass transition temperature (T_g) of the composites (Fig. 7). The T_g of recycled PVC was 86.7 °C, which decreased by 2.8–4 °C in the composites. This was

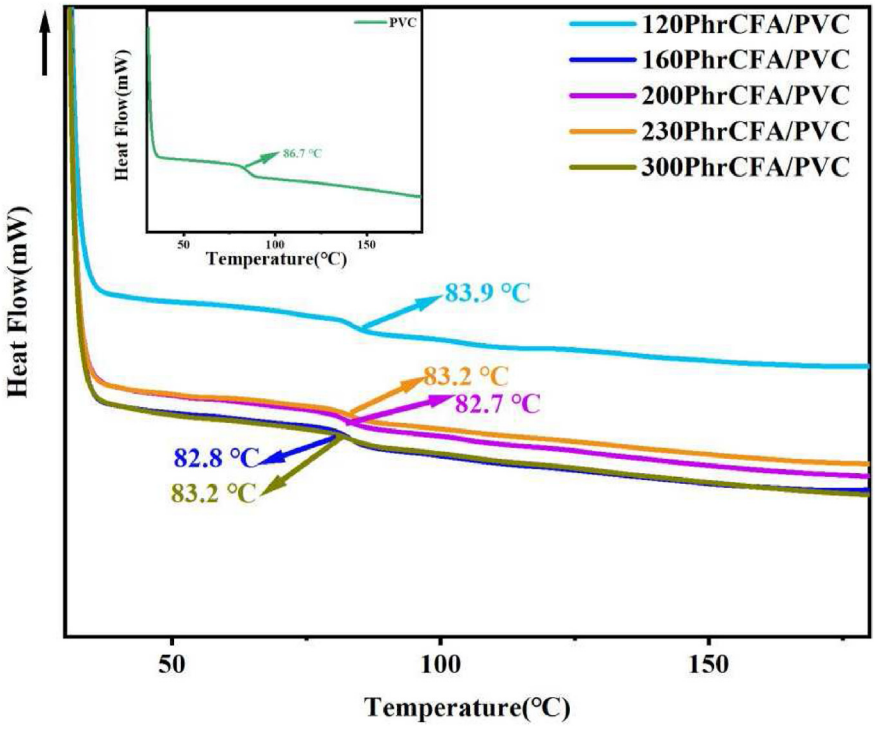

Fig. 7 – DSC curves of the CFA/PVC composites.

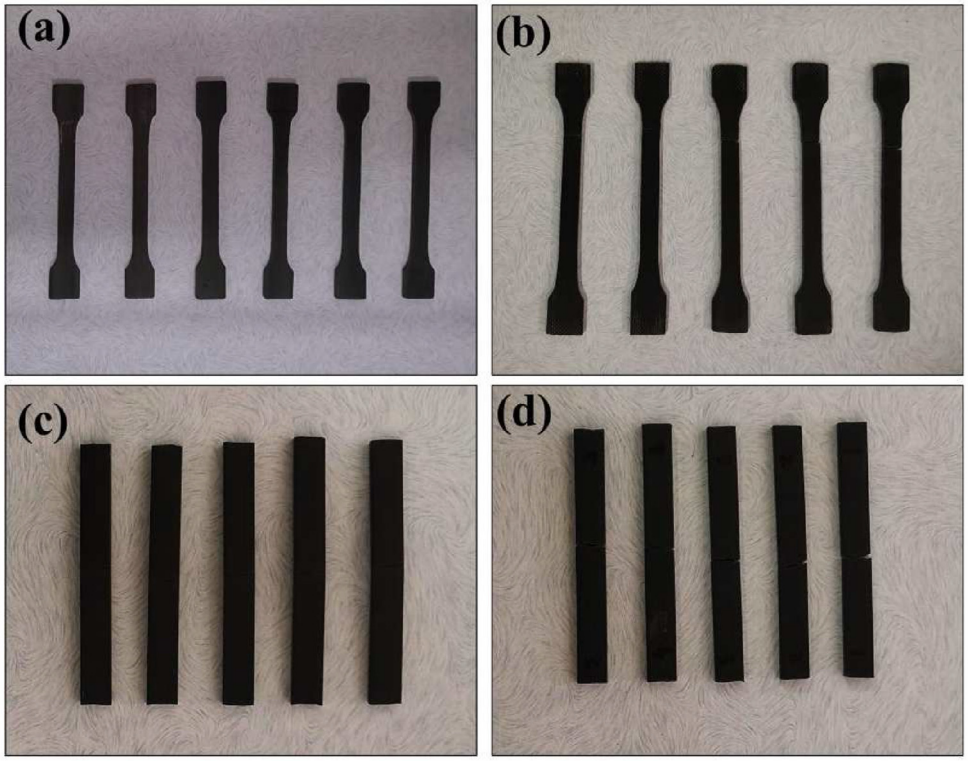

Fig. 8 – Samples before (a) and after (b) the tension strength measurement; (b) samples after the bending strength measurement; (d) samples after the impact strength test.

attributed to the addition of some additives during the processing. Nevertheless, the decrease in T_g does not affect the practical use of our materials.

3.3. *Practical application of the composites*

Mechanical properties are critical for our materials to be used as decking boards; therefore, we systematically measured the performance of our materials under stretching, bending, impact strength and hardness. The test samples are shown in Fig. 8, and the results in Fig. 9 and Table 5.

The bending strength of the composites were determined to be 42, 34.9 and 31.3 MPa, for 120PhrCFA/PVC, 200PhrCFA/PVC and 300PhrCFA/PVC, respectively, by measuring their strain–stress curves (Fig. S3). The reduction in bending strength was attribute to the aggregation of CFA particles at high CFA content that reduce the interaction between CFA and PVC in the composites. Nevertheless, the bending modulus increased with increasing CFA content (Fig. 9a), which was due to the rigidity of CFA that restricts the mobility of PVC chains under loading.

The impact strength of the composites decreases with increasing CFA content, which is consisted with previous reports [3]. The impact strength decrease of 120PhrCFA/PVC was 17.8 kJ/m^2, which decreased to 10.6 and 10.7 kJ/m^2 when the CFA content increased to 200 and 230 parts, respectively. Nevertheless, no rupture of samples was observed in these measurements. However, for the 300PhrCFA/PVC, the sample ruptured during the drop impact and the impact strength reduced to 6.4 kJ/m^2. The reduction in impact strength can also be explained by the low aspect ratio of CFA particles and the reduced binding between CFA and PVC chains as CFA aggregate.

We also measured the Rockwell hardness of the composites (Fig. 9c). The hardness increases from 85.2 to 103 when the CFA content increased from 120 parts to 200 parts, which was attribute to the high rigidity of CFA particles. However, further increase in CFA content to 300 parts decreased the hardness by 12.5%. This might be because of the formation of CFA aggregates that cause the in-homogeneous distribution of stress under loading and the reduced interaction between CFA particles and PVC chains.

We further characterized the tension strength of the composites (Fig. 9d and Fig. S4). The result of the tension strength ranged from 15.1 to 17.2 MPa when composites with CFA content increased from 120 to 230 parts. However, the tension strength dropped down to 11.3 MPa when the CFA content further increased to 300 parts. Therefore, the maximum CFA content for the composites was 200 parts.

More importantly, according to our estimation, our strategy could save around 500 CNY (Chinese Yuan) per tons of decking, reducing the cost by about 10–20%. The use of CFA as alternative to $CaCO_3$ in producing decking not only reduces the negative impact of CFA, but also reduce the economic cost of the decking (Fig. S5) without compromise in the mechanical properties.

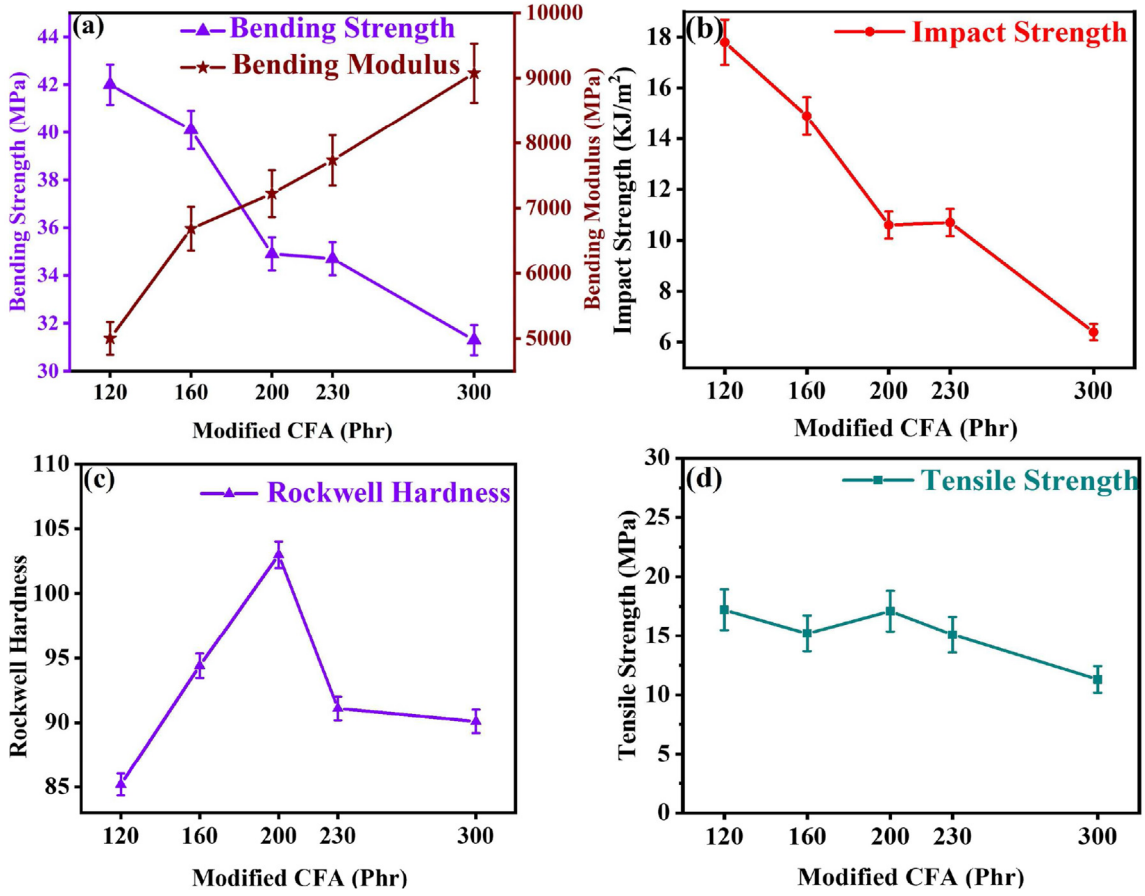

Fig. 9 – (a) Bending strength and bending modulus, (b) impact strength, (c) hardness (HRR) and (d) tensile strength of the composites.

Table 5 – Mechanical properties of modified CFA/PVC composites with different content.

Sample	Bending strength (MPa)	Bending modulus (MPa)	Impact strength (KJ/m^2)	Hardness (HRR)	Tensile strength (MPa)
120PhrCFA/PVC	42.0 ± 0.84	5003 ± 305	17.8 ± 1.00	85.2 ± 0.80	17.2 ± 1.80
160PhrCFA/PVC	40.1 ± 0.80	6684 ± 430	14.9 ± 0.90	94.4 ± 0.90	15.2 ± 1.75
200PhrCFA/PVC	34.9 ± 0.70	7223 ± 577	10.6 ± 0.60	103 ± 1.10	17.1 ± 1.83
230PhrCFA/PVC	34.7 ± 0.70	7736 ± 570	10.7 ± 0.53	91.1 ± 1.00	15.1 ± 1.68
300PhrCFA/PVC	31.3 ± 0.63	9077 ± 630	6.4 ± 0.32	90.1 ± 0.95	11.3 ± 0.90

In addition, because of the simplicity of our procedure, the whole process has been industrialized. Therefore, we expect that our research could be readily transformed to commercial products.

4. Conclusion

In summary, we reported a simple process that converts the coal fly ash (CFA) to high performance CFA/polyvinyl chloride (PVC) composites for decking. To improve the compatibility of CFA with the PVC, we adopted an in-situ modification strategy that could avoid the possible dust pollution in conventional multistep procedures. The effectiveness of our strategy was confirmed by a serious of characterization. The resulting composites exhibited excellent mechanical performance. Critically, the bending strength, bending modulus, impact strength, hardness and waterproof performance of our composites with high CFA content met or exceed the industrial standard. More importantly, our estimation suggested that, our strategy could reduce the cost for production of decking by 10–20%.

Funding sources

This work was supported by Key Research and Development Program of Ningxia [Grant Nos. 2022BDE02001 and

2022BDE03003], Fundamental Research Funds for the Central Universities, North Minzu University [Grant No. 2020KYQD32], Key Research and Development Program (Talents Project) of Ningxia [Grant No. 2021BEB04067], and the Natural Science Foundation of Ningxia [Grant No. 2022AAC03220].

CRediT authorship contribution statement

Shengwei Guo and Dan Li: conceptualization, methodology, funding acquisition, writing-review and editing; **Guxia Wang:** writing-review and editing, formal analysis; **Jun Yan, Yongqiang Qian and Yan Wei:** writing-review and editing, investigation; Zhaoshuai Li: writing-original draft, investigation, formal analysis.

Declaration of Competing Interest

The authors declare that they have no known competing financial interests or personal relationships that could have appeared to influence the work reported in this paper.

Appendix A. Supplementary data

Supplementary data to this article can be found online at https://doi.org/10.1016/j.jmrt.2023.02.026.

REFERENCES

[1] Luo Y, Wu Y, Ma S, Zheng S, Zhang Y, Chu PK. Utilization of coal fly ash in China: a mini-review on challenges and future directions. Environ Sci Pollut Res 2021;28:18727–40. https://doi.org/10.1007/s11356-020-08864-4.

[2] Yao ZT, Ji XS, Sarker PK, Tang JH, Ge LQ, Xia MS, et al. A comprehensive review on the applications of coal fly ash. Earth Sci Rev 2015;141:105–21. https://doi.org/10.1016/j.earscirev.2014.11.016.

[3] Li Y, Lv L, Wang W, Zhang J, Lin J, Zhou J, et al. Effects of chlorinated polyethylene and antimony trioxide on recycled polyvinyl chloride/acryl-butadiene-styrene blends: flame retardancy and mechanical properties. Polymer 2020;190. https://doi.org/10.1016/j.polymer.2020.122198.

[4] Feng W, Wan Z, Daniels J, Li Z, Xiao G, Yu J, et al. Synthesis of high quality zeolites from coal fly ash: mobility of hazardous elements and environmental applications. J Clean Prod 2018;202:390–400. https://doi.org/10.1016/j.jclepro.2018.08.140.

[5] Qi L, Yao Y, Han T, Li J. Research on the electrostatic characteristic of coal-fired fly ash. Environ Sci Pollut Res 2019;26:7123–31. https://doi.org/10.1007/s11356-019-04166-6.

[6] Zhang P, Tian X, Fu D. CO2 removal in tray tower by using AAILs activated MDEA aqueous solution. Energy 2018;161:1122–32. https://doi.org/10.1016/j.energy.2018.07.162.

[7] Qi L, Li J, Yao Y, Zhang Y. Heavy metal poisoned and regeneration of selective catalytic reduction catalysts. J Hazard Mater 2019;366:492–500. https://doi.org/10.1016/j.jhazmat.2018.11.112.

[8] Peng B, Guo D, Qiao H, Yang Q, Zhang B, Hayat T, et al. Bibliometric and visualized analysis of China's coal research 2000–2015. J Clean Prod 2018;197:1177–89. https://doi.org/10.1016/j.jclepro.2018.06.283.

[9] Wang D, Wan K, Yang J. Measurement and evolution of eco-efficiency of coal industry ecosystem in China. J Clean Prod 2019;209:803–18. https://doi.org/10.1016/j.jclepro.2018.10.266.

[10] Wang X, Fu C, Feng Z, Huo H, Yin X, Gao G, et al. Fly ash/polymer composite electrolyte with internal binding interaction enables highly-stable extrinsic-interfaces of all-solid-state lithium batteries. Chem Eng J 2022;428. https://doi.org/10.1016/j.cej.2021.131041.

[11] Jayaranjan MLD, van Hullebusch ED, Annachhatre AP. Reuse options for coal fired power plant bottom ash and fly ash. Rev Environ Sci Biotechnol 2014;13:467–86. https://doi.org/10.1007/s11157-014-9336-4.

[12] Lu C-f, Wang W, Li Q-t, Hao M, Xu Y. Effects of micro-environmental climate on the carbonation depth and the pH value in fly ash concrete. J Clean Prod 2018;181:309–17. https://doi.org/10.1016/j.jclepro.2018.01.155.

[13] Mo L, Zhang F, Panesar DK, Deng M. Development of low-carbon cementitious materials via carbonating portland cement–fly ash–magnesia blends under various curing scenarios: a comparative study. J Clean Prod 2017;163:252–61. https://doi.org/10.1016/j.jclepro.2016.01.066.

[14] Wu J, Bai G-l, Zhao H-y, Li X. Mechanical and thermal tests of an innovative environment-friendly hollow block as self-insulation wall materials. Construct Build Mater 2015;93:342–9. https://doi.org/10.1016/j.conbuildmat.2015.06.003.

[15] Shi Y, Li Y, Tang Y, Yuan X, Wang Q, Hong J, et al. Life cycle assessment of autoclaved aerated fly ash and concrete block production: a case study in China. Environ Sci Pollut Res 2019;26:25432–44. https://doi.org/10.1007/s11356-019-05708-8.

[16] Wang L, Sun H, Sun Z, Ma E. New technology and application of brick making with coal fly ash. J. Mater. J. Mater. Cycles Waste Manage. 2015;18:763–70. https://doi.org/10.1007/s10163-015-0368-9.

[17] Zhao S, Song K, Zhu J, Ma D, Shi J-W. Gd-Mn-Ti composite oxides anchored on waste coal fly ash for the low-temperature catalytic reduction of nitrogen oxide. Separ Purif Technol 2022;302:122119. https://doi.org/10.1016/j.seppur.2022.122119.

[18] Qi L, Xu J, Liu K. Porous sound-absorbing materials prepared from fly ash. Environ Sci Pollut Res 2019;26:22264–72. https://doi.org/10.1007/s11356-019-05573-5.

[19] Czarna-Juszkiewicz D, Cader J, Wdowin M. From coal ashes to solid sorbents for hydrogen storage. J Clean Prod 2020;270. https://doi.org/10.1016/j.jclepro.2020.122355.

[20] Xiu F-R, Yu X, Qi Y. A high-efficiency and low-temperature subcritical water dechlorination strategy of polyvinyl chloride using coal fly ash (CFA) and coal gangue (CG) as enhancers. J Clean Prod 2020;260. https://doi.org/10.1016/j.jclepro.2020.121085.

[21] Bora PJ, Porwal M, Vinoy KJ, Kishore, Ramamurthy PC, Madras G. Industrial waste fly ash cenosphere composites based broad band microwave absorber. Composites, Part B 2018;134:151–63. https://doi.org/10.1016/j.compositesb.2017.09.062.

[22] Atun G, Ayar N, Kurtoglu AE, Ortaboy S. A comparison of sorptive removal of anthraquinone and azo dyes using fly ash from single and binary solutions. J Hazard Mater 2019;371:94–107. https://doi.org/10.1016/j.jhazmat.2019.03.006.

[23] Janos P, Buchtova H, Ryznarova M. Sorption of dyes from aqueous solutions onto fly ash. Water Res 2003;37:4938–44. https://doi.org/10.1016/j.watres.2003.08.011.

[24] Adamczuk A, Kołodyńska D. Equilibrium, thermodynamic and kinetic studies on removal of chromium, copper, zinc and arsenic from aqueous solutions onto fly ash coated by chitosan. Chem Eng J 2015;274:200–12. https://doi.org/10.1016/j.cej.2015.03.088.
[25] Yu J, Sun L, Ma C, Qiao Y, Yao H. Thermal degradation of PVC: a review. Waste Manage (Tucson, Ariz) 2016;48:300–14. https://doi.org/10.1016/j.wasman.2015.11.041.
[26] Jeamtrakull S, Kositchaiyong A, Markpin T, Rosarpitak V, Sombatsompop N. Effects of wood constituents and content, and glass fiber reinforcement on wear behavior of wood/PVC composites. Composites, Part B 2012;43:2721–9. https://doi.org/10.1016/j.compositesb.2012.04.031.
[27] Poltabtim W, Wimolmala E, Markpin T, Sombatsompop N, Rosarpitak V, Saenboonruang K. X-Ray shielding, mechanical, physical, and water absorption properties of wood/PVC composites containing bismuth oxide. Polymers 2021;13. https://doi.org/10.3390/polym13132212.
[28] Liu H, Wang J, Wen S, Gong C, Zheng G, Xiong C, et al. Processability, morphology, thermal, and mechanical properties of rigid PVC composites with liquid macromolecular modifier-coated $CaCO_3$. Polym Compos 2015;36:1286–92. https://doi.org/10.1002/pc.23033.
[29] Schneider H, Fischer R, Schreuer J, Green D. Mullite: crystal structure and related properties. J Am Ceram Soc 2015;98:2948–67. https://doi.org/10.1111/jace.13817.
[30] Feng Y, Chen H, Dong X, Qu J, He H, Xu B, et al. Polyvinyl alcohol-modified Pithecellobium Clypearia Benth herbal residue fiber/polypropylene composites. Polym Compos 2016;37:915–24. https://doi.org/10.1002/pc.23250.
[31] Jin Y, Wang E, Weng Y, Men S, Dong Y, Sima Y, et al. The investigation of the toughening mechanism of PHBV/PBAT with a novel hyperbranched ethylenediamine triazine polymer based modifier: the Formation of the transition layer and the microcrosslinking structure. J Polym Environ 2018;26:4158–67. https://doi.org/10.1007/s10924-018-1286-4.
[32] Yu Z, Gao Y, Jiang J, Gu H, Lv S, Ni H, et al. Study on effects of FDM 3D printing parameters on mechanical properties of polylactic acid. IOP Conf Ser Mater Sci Eng 2019;688:033026. https://doi.org/10.1088/1757-899x/688/3/033026.
[33] Qin W, He J, Meng J. Research on composite powder and magnet properties of bonded NdFeB magnets. Adv Mater Res 2012;535–537:1314–8. https://doi.org/10.4028/www.scientific.net/AMR.535-537.1314.
[34] Gong W, Gao J, Jiang M, He L, Yu J, Zhu J. Influence of cell structure parameters on the mechanical properties of microcellular polypropylene materials. J Appl Polym Sci 2011;122:2907–14. https://doi.org/10.1002/app.33874.
[35] Gong W, Jiang T-H, Zeng X-B, He L, Zhang C. Experimental-numerical studies of the effect of cell structure on the mechanical properties of polypropylene foams. E-Polymers 2020;20:713–23. https://doi.org/10.1515/epoly-2020-0060.
[36] Xue X, Liu Y-L, Dai J-G, Poon C-S, Zhang W-D, Zhang P. Inhibiting efflorescence formation on fly ash–based geopolymer via silane surface modification. Cem Concr Compos 2018;94:43–52. https://doi.org/10.1016/j.cemconcomp.2018.08.013.
[37] Khan MZ, Baheti V, Militky J, Ali A, Vikova M. Superhydrophobicity, UV protection and oil/water separation properties of fly ash/trimethoxy(octadecyl)silane coated cotton fabrics. Carbohydr Polym 2018;202:571–80. https://doi.org/10.1016/j.carbpol.2018.08.145.
[38] van der Merwe EM, Mathebula CL, Prinsloo LC. Characterization of the surface and physical properties of South African coal fly ash modified by sodium lauryl sulphate (SLS) for applications in PVC composites. Powder Technol 2014;266:70–8. https://doi.org/10.1016/j.powtec.2014.06.008.
[39] Jia Y, Feng H, Shen D, Zhou Y, Chen T, Wang M, et al. High-performance microbial fuel cell anodes obtained from sewage sludge mixed with fly ash. J Hazard Mater 2018;354:27–32. https://doi.org/10.1016/j.jhazmat.2018.04.008.
[40] van der Merwe EM, Prinsloo LC, Mathebula CL, Swart HC, Coetsee E, Doucet FJ. Surface and bulk characterization of an ultrafine South African coal fly ash with reference to polymer applications. Appl Surf Sci 2014;317:73–83. https://doi.org/10.1016/j.apsusc.2014.08.080.
[41] Li Y, Min X, Ke Y, Liu D, Tang C. Preparation of red mud-based geopolymer materials from MSWI fly ash and red mud by mechanical activation. Waste Manage (Tucson, Ariz) 2019;83:202–8. https://doi.org/10.1016/j.wasman.2018.11.019.
[42] Patil AG, Anandhan S. Influence of planetary ball milling parameters on the mechano-chemical activation of fly ash. Powder Technol 2015;281:151–8. https://doi.org/10.1016/j.powtec.2015.04.078.
[43] Patil AG, Shanmugharaj AM, Anandhan S. Interparticle interactions and lacunarity of mechano-chemically activated fly ash. Powder Technol 2015;272:241–9. https://doi.org/10.1016/j.powtec.2014.12.006.
[44] Ye C, Yan B, Ji X, Liao B, Gong R, Pei X, et al. Adsorption of fluoride from aqueous solution by fly ash cenospheres modified with paper mill lime mud: experimental and modeling. Ecotoxicol Environ Saf 2019;180:366–73. https://doi.org/10.1016/j.ecoenv.2019.04.086.
[45] Maurya AK, Gogoi R, Manik G. Study of the moisture mitigation and toughening effect of fly-ash particles on sisal fiber-reinforced hybrid polypropylene composites. J Polym Environ 2021;29:2321–36. https://doi.org/10.1007/s10924-021-02043-3.
[46] Parvaiz MR, Mohanty S, Nayak SK, Mahanwar PA. Effect of surface modification of fly ash on the mechanical, thermal, electrical and morphological properties of polyetheretherketone composites. Mater Sci Eng 2011;528:4277–86. https://doi.org/10.1016/j.msea.2011.01.026.
[47] Xia Z, Yang H, Sun J, Zhou Z, Wang J, Zhang Y. Co-pyrolysis of waste polyvinyl chloride and oil-based drilling cuttings: pyrolysis process and product characteristics analysis. J Clean Prod 2021;318. https://doi.org/10.1016/j.jclepro.2021.128521.
[48] Khoshnoud P, Abu-Zahra N. Kinetics of thermal decomposition of PVC/fly ash composites. Int J Polym Anal Char 2017;23:170–80. https://doi.org/10.1080/1023666x.2017.1404668.
[49] Wang Z, Xie T, Ning X, Liu Y, Wang J. Thermal degradation kinetics study of polyvinyl chloride (PVC) sheath for new and aged cables. Waste Manage (Tucson, Ariz) 2019;99:146–53. https://doi.org/10.1016/j.wasman.2019.08.042.
[50] Sakata Y, Uddin M, Koizumi K, Murata K. Catalytic degradation of polypropylene into liquid hydrocarbons using silica-alumina catalyst. Chem Lett 1996;25:245–6. https://doi.org/10.1246/cl.1996.245.
[51] Ohkita H, Nishiyama R, Tochihara Y, Mizushima T, Kakuta N, Morioka Y, et al. Acid properties of silica-alumina catalysts and catalytic degradation of polyethylene. Ind Eng Chem Res 1993;32:3112–6. https://doi.org/10.1021/ie00024a021.
[52] Uddin M, Sakata Y, Shiraga Y, Muto A, Murata K. Dechlorination of chlorine compounds in poly (vinyl chloride) mixed plastics derived oil by solid sorbents. Ind Eng Chem Res 1999;38:1406–10. https://doi.org/10.1021/ie980445k.
[53] Hapipi AM, Suda H, Uddin MA, Kato Y. Dechlorination of polyvinyl chloride under superheated steam with catalysts and adsorbents. Energy Fuels 2018;32:7792–9. https://doi.org/10.1021/acs.energyfuels.8b00838.